Experimental and simulation analysis of community structure of nitrifying bacteria in a membrane-aerated biofilm

S. Matsumoto*, A. Terada*, Y. Aoi*, S. Tsuneda*, E. Alpkvist, C. Picioreanu*** and M.C.M. van Loosdrecht*****

*Department of Chemical Engineering, Waseda University, Ohkubo 3-4-1, Shinjuku-ku, Tokyo 169-8555, Japan

**Applied Mathematics Group, School of Technology and Society, Malmö University, SE-205 06 Malmö, Sweden

***Department of Biotechnology, Delft University of Technology, Julianalaan 67, 2628 BC Delft, The Netherlands

Abstract Until now, only few attempts have been made to assess biofilm models simulating microenvironments in a biofilm. As a first step, we compare the microenvironment observed in a membrane aerated biofilm (MAB) to that derived from a two-dimensional computational model with individual ammonia oxidizing bacteria (AOB) and nitrite oxidizing bacteria (NOB) embedded in a continuum EPS matrix. Gradients of oxygen were determined by means of microelectrodes. The change in nitrifying bacterial populations with the biofilm depth was quantified using fluorescence *in situ* hybridization (FISH) in combination with a confocal laser scanning microscopy (CLSM). Microelectrode measurements revealed that oxic and anoxic or anaerobic regions exist within the MAB. The oxygen profile predicted by the model showed good agreement with that obtained by microelectrode measurements. The oxic part of the biofilm was dominated by NSO190 probe-hybridized AOB, which formed relatively large clusters of cells directly on the membrane surface, and by the NOB belonging to genus *Nitrobacter* sp. On the other hand, NOB belonging to genus *Nitrospira* sp. were abundant at the oxic-anoxic interface. The model prediction regarding AOB and *Nitrobacter* sp. distribution was consistent with the experimental counterpart. Measurements of AOB cluster size distribution showed that colonies are slightly larger adjacent to the membrane than at the inner part of the biofilm. The sizes predicted by the current model are larger than those obtained in the experiment, leading to the arguments that some factors not contained in the model would affect the cluster size.

Keywords Biofilm model; fluorescence *in situ* hybridization (FISH); membrane-aerated biofilm reactor (MABR); two-dimensional

Water Science & Technology **Vol 55 No 8–9 pp 283–290** © IWA Publishing 2007

Introduction

Community structure of various microorganisms in biofilms is an important factor in determining the effectiveness of biological nitrogen removal in industrial and municipal wastewater treatment systems (Cole *et al.*, 2004). In biological nitrogen removal, ammonia nitrogen in wastewater is removed through two steps – an aerobic nitrification and a subsequent anoxic denitrification. Nitrogen removal has conventionally been achieved via two separate reactors in series. Recent works have emphasized the effectiveness of a membrane-aerated biofilm reactor (MABR) in that it allows simultaneous nitrification and denitrification (SND) in a biofilm (Hibiya *et al.*, 2003; Semmens *et al.*, 2003; Terada *et al.*, 2003). In the MABR, oxygen for bacterial growth and maintenance is supplied from the lumen of a gas-permeable membrane. Oxygen diffuses through the biofilm, facilitating the growth of biomass on the membrane shell. Other substrates diffuse into the biofilm from the bulk liquid within which the membrane is suspended. Such a structure with counter-diffusion of substrates allows several different reactions to be accomplished in a single biofilm: nitrification is achieved in the oxygen-rich zone close

doi: 10.2166/wst.2007.269

to the membrane outer surface, whereas denitrification occurs in the substrate-rich anoxic zone close to the top of the biofilm, thereby ensuring SND in the biofilm. For the practical application of an MABR, it is necessary to both understand and ultimately control the microenvironment in the biofilm, which leads to manipulation of optimal community structure and spatial organization in the biofilm and consequently high nitrogen removal efficiency.

Computational models capable of describing biofilm structure and microenvironments in two or three spatial dimensions have been recently developed, exhibiting intriguing insights with regard to structural and microbial biofilm heterogeneity (Picioreanu *et al.*, 1998, 2004). A recent model can especially express behaviour of extracellular polymeric substance (EPS) in a biofilm, showing cluster formation by nitrifying bacteria (Alpkvist *et al.*, 2006). However, most of these modeling results have not been directly compared to a detailed experimental analysis of microbial communities in biofilms. This study was therefore undertaken to directly compare experimental with modeling results regarding population distributions and cluster size of nitrifying bacteria in a membrane-aerated biofilm (MAB).

Materials and methods

Biofilm model

The basic approach used by the 2-d computational biofilm model is described in detail in Alpkvist *et al.* (2006). The model represents the biofilm by combined interactions between discrete biomass particles (e.g. individual cells) using an individual-based approach (Kreft *et al.*, 2001) and a continuum field describing the EPS matrix (Alpkvist *et al.*, 2006). In the individual-based biomass description, ammonia-oxidizing bacteria (AOB), nitrite-oxidizing bacteria (NOB), heterotrophic bacterial (HB) and inert biomass are spherical entities with an internal state defined by their composition (mass of one or more particulate substances), size and location in space. The particles imitate the behaviour of a microbial cell: they grow by uptake of nutrients and divide creating an offspring particle. EPS is excreted by HB but not by either AOB or NOB. On the other hand, the EPS matrix is described as an incompressible viscous fluid, which can expand and shrink due to generation and consumption processes. The particles are assumed to move by a specific pushing mechanism and by an advective mechanism supported by the EPS dynamics. Detachment of both cells and EPS matrix follows a continuum approach.

Biofilm reactor operation

MABs were grown in a rectangular and closed flow-cell reactor with a working volume of 3.0 L (6 cm width, 6 cm height and 1 m length) and membrane surface area of 36 cm^2. Substrates with 100 g/m^3 chemical oxygen demand (COD) and 50 g/m^3 ammonia nitrogen were continuously fed in the reactor at a hydraulic retention time of 24 h. Oxygen was supplied at an air pressure of 10 kPa through the membrane. Temperature was controlled at approximately 23 °C and an average fluid velocity was set at 5 cm/s. Biofilm samples (dimension: 1 × 1 cm) were taken from the reactor 26 days after the start-up.

Microelectrode measurement

Dissolved oxygen (DO) profiles were obtained with a Clark-type microelectrode with a tip diameter of 10–15 μm (Unisense, Aarhus, Denmark). MAB was transferred into a flow cell with a volume of 1 L for measurements of DO concentration. The same flow rate of 5 cm/s was employed in the measurement flow cell. The biofilm samples taken from the reactor were exposed in a medium having the same substrate composition with

that used for the reactor operation for a few hours before the measurement to ensure that steady-state concentration profiles were obtained.

Fixation and cryosectioning of biofilm samples

After the microelectrode measurement, a part of the biofilm was sampled and immediately fixed with freshly prepared 4% paraformaldehyde solution for 18 h at 4 °C. The sample was embedded in OCT compound (Tissu-Tek, Sakura Finetek, Tokyo, Japan) overnight to infiltrate the OCT compound into the biofilm, as described by Aoi *et al.* (2000). After rapid freezing at −21 °C, 20 μm thick vertical slices were prepared with a cryostat (CM1850, Leica, Heidelderg, Germany) and placed on a gelatin-coated slide (Matsunami, Osaka, Japan). After air drying overnight, the slices were dehydrated by successive passage through 50, 80 and 98% ethanol washes (for 3 min each), air dried, and stored at room temperature.

In situ hybridization

The sequences of all oligonucleotide probes used in this study are given in Table 1. Probes were synthesized and fluorescently labeled with fluorescein isothiocyanate (FITC) and the hydrophilic sulphoindocyanine dyes Cy3 at the 5′ end. All *in situ* hybridization were performed according to the protocol by Amann *et al.* (1990) in hybridization buffer (0.9 M NaCl, 20 mM Tris hydrochloride (pH 7.2), 0.01% sodium dodecyl sulfate (SDS), formamide whose concentrations are listed in Table 1) at 46 °C for 2 to 3 h. Subsequently, a stringent washing step was performed at 48 °C for 15 min in 50 ml of washing solution (NaCl (dependent on FA concentration) 20 mM Tris hydrochloride (pH 7.2), 0.01% SDS). The slides were then rinsed briefly with ddH_2O and then allowed to dry. Slides were mounted in FluoroGuard Antifade Reagent (Bio-Rad, CA, USA). A confocal laser scanning microscope (CLSM; IX71, Olympus, Tokyo, Japan) equipped with an Ar ion laser (488 nm) and a HeNe laser (543 nm) was used to detect and record probe-stained cells.

Nitrifying bacterial cell and AOB cluster size distribution

Nitrifying populations with biofilm depth were quantified by processing the CLSM images. Threshold values were defined to exclude background fluorescence. Each 50 μm layer of the biofilm, starting at the membrane surface, was quantified to evaluate the probe-positive cell area. The size distribution of AOB clusters was manually measured along vertical transects through the biofilms. The average cell counts and cluster sizes were determined by 5 representative CLSM images of each cross section of the biofilm samples. Comparisons of experimental results with model predictions were performed based on dimensionless biofilm thickness because each biofilm sample has different thickness.

Table 1 Probe sequences and formamide concentration in the hybridization buffer required for specific in situ hybridization

Probe	Specificity	Sequence of Probe (5′ to 3′)	FA (%)[a]	Reference
EUB338	Most bacteria	GCTGCCTCCCGTAGGAGT	–[b]	Amann *et al.*, 1990
Nso190	Ammonia-oxidizing *β*-proteobacteria	CGATCCCCTGCTTTTCTCC	35[c]	Mobarry *et al.*, 1996
Ntspa1026	*Nitrospira moscoviensis*	AGCACGCTGGTATTGCTGC	20	Juretschko *et al.*, 1998
NIT3	*Nitrobacter* spp.	CCTGTGCTCCATGCTCCG	40	Wagner *et al.*, 1995

[a]Formamide concentration in the hybridization buffer
[b]Used at any formamide concentration
[c]Although originally 55% formamide should be used, we referred to Pynaert *et al.* (2003)

Results and discussion

Simulation results

The simulation results of 2-d MAB growth in time are shown in Figure 1. The simulation was conducted at the same substrate concentrations with the experiment (i.e. COD of 100 g/m^3 and ammonia nitrogen of 50 g/m^3). All kinetic and stoichiometric parameters were determined in the range according to Alpkvist *et al.* (2006), Kindaichi *et al.* (2006) and Picioreanu *et al.* (2004). EPS production caused by heterotrophic bacterial growth leads to sparse distribution of HB in the biofilm. Since AOB and NOB are not assumed to produce EPS, AOB and NOB cells aggregate into spherical clusters and the clusters are surrounded by the EPS matrix (on day 15 and 26 in Figure 1). The bacterial population profiles indicates the feasibility of simultaneous COD and T-N removal within the MAB: AOB and NOB can grow at the base of the biofilm where oxygen concentration is the highest and consume the oxygen supplied through the membrane; on the other hand, HB dominate the region adjacent to the bulk liquid where oxygen is depleted and consume COD as an electron donor and nitrite or nitrate as an electron acceptor at the anoxic region, resulting in SND (Figures 1 and 2A). This result has the same trend with the results experimentally observed in other reports (Terada *et al.*, 2003; Cole *et al.*, 2004).

DO profiles within MAB

DO is considered to play an essential role especially for controlling the nitrifying bacterial microenvironment within biofilms (Okabe *et al.*, 1999, 2004; Schramm *et al.*, 2000). Figure 3 shows the comparison of DO profiles in the experiment with model prediction. Experimental DO measurements show, as expected, that oxic and anoxic or anaerobic regions were created within the biofilm. DO concentration at the membrane surface was about 8.0 mg/l. At the biofilm surface, a little amount of DO was detected (0.2 mg/l) probably due to oxygen dissolution form the bulk liquid. The model prediction agrees well quantitatively with the experimental result.

Comparison of experimental observation with model prediction on nitrifying bacterial distribution

Figure 4A presents the distributions of Nso190 probe-hybridized AOB within the biofilm. Microscopic observations showed that the number of AOB was the largest at the membrane surface, decreasing then toward the top of the biofilm, accompanied with decreasing in DO concentration. AOB were detected at the biofilm surface in concordance with an increase in DO concentration (Figure 3). The model prediction of AOB distribution

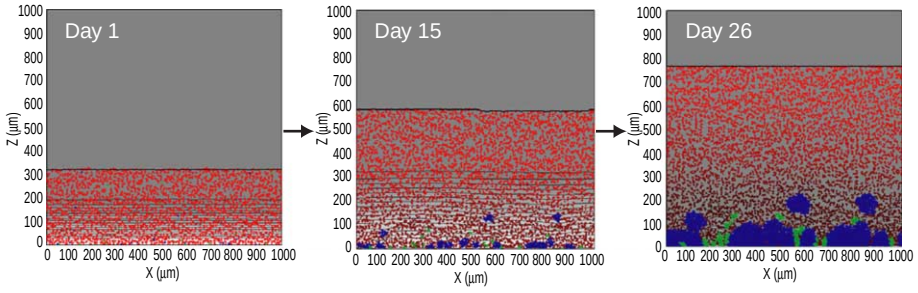

Figure 1 Simulation results of 2-d MAB development at different moments in time. Red, blue and green dots are heterotrophic bacteria (HB), ammonia-oxidizing bacteria (AOB) and nitrite-oxidizing bacteria (NOB), respectively. The brightness of color increases with an increase in bacterial activity. Contour lines and gray shades show a gradual decrease in DO from the highest value near the membrane (white) to the lowest value near the biofilm surface (dark gray). Subscribers to the online version of *Water Science and Technology* can access the colour version of this figure from http://www.iwaponline.com/wst

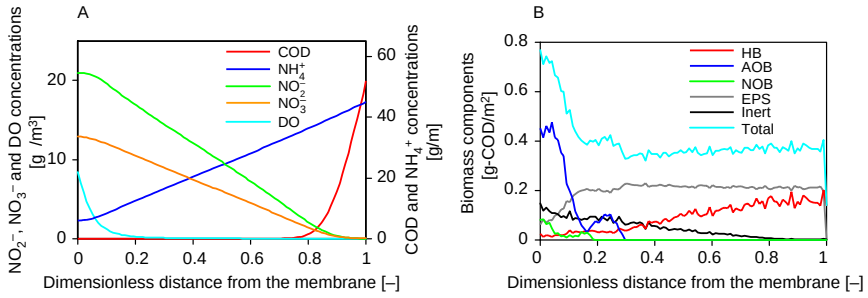

Figure 2 Simulation profiles of horizontally averaged values for substrates and biomass components along the biofilm depth on day 26: chemical profiles (A) and the amount of biomass component (B). Subscribers to the online version of *Water Science and Technology* can access the colour version of this figure from http://www.iwaponline.com/wst

showed good agreement with the experimental data, indicating that the 2-d biofilm model in this study can effectively predict the behaviour of AOB growth.

The distributions of NOB within the biofilm are shown in Figure 4B. This graph shows two different groups of NOB, i.e. *Nitrospira* and *Nitrobacter*, both of which were detected by probes of Ntspa1026 and NIT3, respectively. *Nitrobacter* sp. showed preference for the high DO concentration at the base of the biofilm. As oxygen concentration decreased in the direction of the bulk liquid, the cell numbers of *Nitrobacter* decreased. On the other hand, *Nitrospira*, which was not abundant at the base of the biofilm, was detected at the middle part of the biofilm. Taking into account the reports that *Nitrobacter* has a high growth rate and low affinity for oxygen, whereas *Nitrospira* is inhibited by high oxygen concentration (Okabe *et al.*, 1999; Schramm *et al.*, 2000), the obtained results support such theoretical explanation. These results obviously indicated these two types of NOB inhabited different regions in the biofilm. The model can predict the behaviour of *Nitrobacter* but not *Nitrospira*. In this model setup, the inhibition of *Nitrospira* by high levels of oxygen is not considered. To be able to describe this, a further separation of NOB types will be in a future model refinement, with one NOB type necessitating the addition of an O_2 inhibition term in the growth rate. Furthermore, in a 2-d

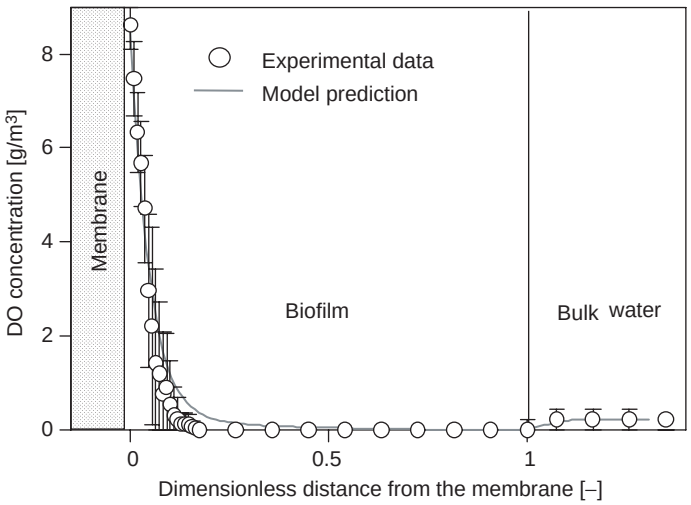

Figure 3 Comparison of DO micro profiles of experimental data with model prediction. Mean value and standard deviations out of five replicates are shown in the experimental result

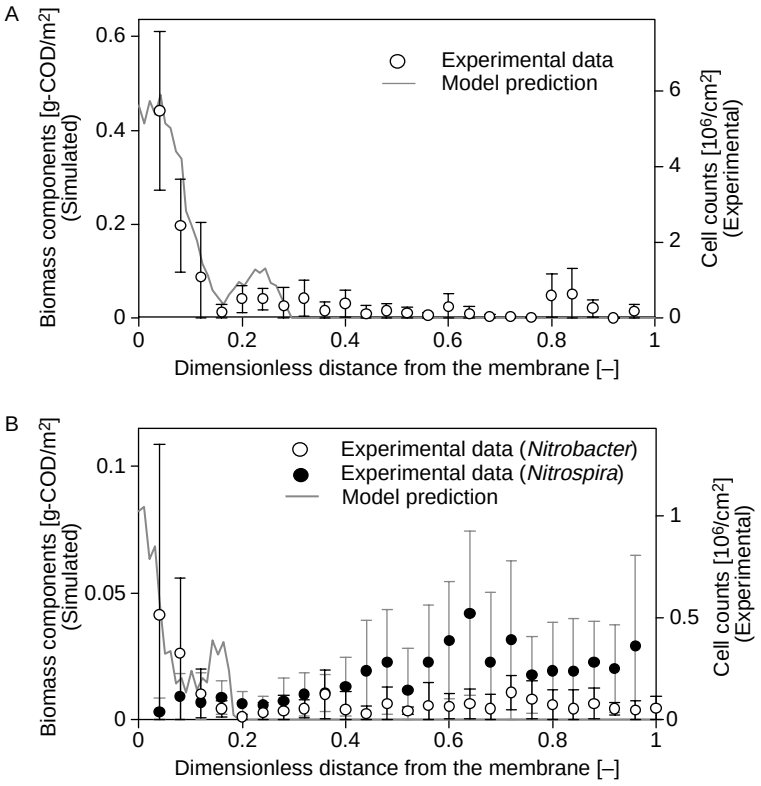

Figure 4 Comparison of experimental data with model prediction regarding (A) AOB and (B) NOB distributions. Experimental result was quantified every 50 μm thickness starting at the membrane (the left side). Measurements were conducted five times and error bars show standard deviation. Note different scale in Y-axis

simulation of a multispecies biofilm community like the one employed in this study, it has been previously reported (Kreft *et al.*, 2001) that the development of the dominant species is less sensitive to parameter values, while the growth of the less abundant species is considerably more sensitive. Indeed, as shown in Figure 4B, the discrepancies between experimental and modeling results regarding less abundant bacteria (NOB) are more significant than those of dominant bacteria (AOB; Figure 4A), which is in concordance with the simulation results reported by Kreft *et al.* (2001).

Comparison of experimental observation with model prediction on the AOB cluster size distribution

Experimental observation of vertical sections of the biofilm revealed that most of the AOB were present as spherical clusters (data not shown). As reported previously (Okabe *et al.*, 2004), substrate concentrations (e.g. DO, NH_4^+ and COD) may affect the size distribution of AOB clusters. Thus, the size distribution of the Nso190 probe-positive AOB clusters was measured (Figure 5). In this study, a group of AOB whose surface area was smaller than 4.9 μm^2 (corresponding to the diameter of 2.5 μm) was not considered as a cluster (Okabe *et al.*, 2004). The horizontal section with less than three clusters was not considered in the analysis. The result shows that the cluster sizes in the experiment are larger near the membrane surface than at the inner part of the biofilm. Some large clusters were also detected at the biofilm surface, but their number was small (data not shown), causing large deviations in the average cluster diameters. It has been reported that the cluster sizes are smaller at the region where COD exists (Okabe *et al.*, 2004).

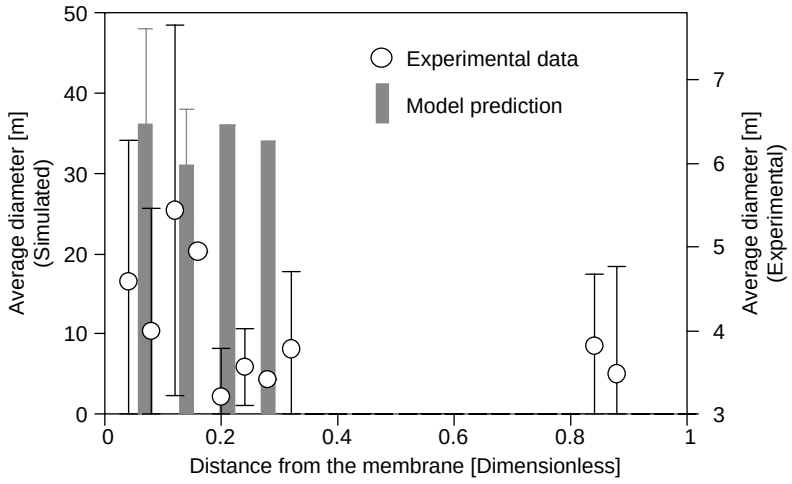

Figure 5 Comparison of experimental AOB distributions with model results. Experimental abundance was quantified in steps of 50 μm starting at the membrane (the left side). Mean value and standard deviations out of five replicates are shown

The difference in the average cluster size in the biofilm is possibly dependent on the gradient of COD concentration in the biofilm. On the other hand, the model predicted much larger cluster sizes than those experimentally observed. This discrepancy suggests that AOB cluster formation may also be regulated other factors not accounted in the model or that model parameters (rate constants and stoichiometry, rate equations) may need readjustments.

Conclusions

The microenvironments predicted by the model clearly indicate the feasibility of simultaneous COD and T-N removal within the MAB. The individual-based model combined with the continuum EPS description generates directly clusters of AOB and NOB, thus allowing for the more precise comparison with experimental results regarding the MAB. DO concentration measurements and distribution profiles of nitrifying bacteria revealed that aerobic and anoxic or anaerobic regions were created within the MAB. Correspondingly, AOB inhabited the aerobic region, which is in agreement with the modeling results. This indicates that the biofilm model used in this study can effectively simulate both microenvironments (e.g. DO profiles) and 2-d microbial distribution (e.g. AOB) within biofilms. Two dominant NOB, i.e. *Nitrobacter* and *Nitrospira*, were detected by FISH. The depth profile of NOB predicted by the model was in better agreement with measured profile for the *Nitrobacter* population rather than with that of *Nitrospira*. This indicates the necessity of the model refinement by further splitting the two NOB groups in different populations. Furthermore, AOB cluster sizes were overestimated by model prediction. This may suggest that either AOB cluster sizes are controlled by unknown factors other than substrate concentration and EPS matrix, or that model parameters must simply be better calibrated. Although remaining model improvement is surely possible, this attempt to quantitatively combine multidimensional modeling with experimental studies will certainly help understanding the development of microbial populations in a complex mixed-species biofilm.

References

Alpkvist, E., Picioreanu, C., van Loosdrecht, M.C.M. and Heyden, A. (2006). Three-dimensional biofilm model with individual cells and continuum EPS matrix. *Biotechnol. Bioeng.*, **94**, 962–979.

Aoi, Y., Miyoshi, T., Okamoto, T., Tsuneda, S., Hirata, A., Kitayama, A. and Nagamune, T. (2000). Microbial ecology of nitrifying bacteria in wastewater treatment process examined by fluorescence in situ hybridization. *J. Biosci. Bioeng.*, **90**(3), 234–240.

Amann, R.I., Krumholz, L. and Stahl, D.A. (1990). Fluorescent-oligonucleotide probing of whole cells for determinative, phylogenetic, and environmental-studies in microbiology. *J. Bacteriol.*, **172**(2), 762–770.

Cole, A.C., Semmens, M.J. and LaPara, T.M. (2004). Stratification of activity and bacterial community structure in biofilms grown on membranes transferring oxygen. *Appl. Environ. Mcrobiol.*, **70**(4), 1982–1989.

Hibiya, A., Terada, A., Tsuneda, S. and Hirata, A. (2003). Simultaneous nitrification and denitrification by controlling vertical and horizontal microenvironment in a membrane-aerated biofilm reactor. *J. Biotechnol.*, **100**(1), 23–32.

Juretschko, S., Timmermann, G., Schmid, M., Schleifer, K.H., Pommerening-Roser, A., Koops, H.P. and Wagner, M. (1998). Combined molecular and conventional analyses of nitrifying bacterium diversity in activated sludge: *Nitrosococcus mobilis* and *Nitrospira*-like bacteria as dominant populations. *Appl. Environ. Microbiol.*, **64**(8), 3042–3051.

Kindaichi, T., Kawano, Y., Ito, T., Satoh, H. and Okabe, S. (2006). Population dynamics and in situ kinetics of nitrifying bacteria in autotrophic nitrifying biofilms as determined by real-time quantitative PCR. *Biotechnol. Bioeng.*, **94**, 1111–1121.

Kreft, J.U., Picioreanu, C., Wimpenny, J.W.T. and van Loosdrecht, M.C.M. (2001). Individual-based modelling of biofilms. *Microbiology*, **147**, 2897–2912.

Mobarry, B.K., Wagner, M., Urbain, V., Rittmann, B.E. and Stahl, D.A. (1996). Phylogenetic probes for analyzing abundance and spatial organization of nitrifying bacteria. *Appl. Environ. Microbiol.*, **62**(6), 2156–2162.

Okabe, S., Satoh, H. and Watanabe, Y. (1999). In situ analysis of nitrifying biofilms as determined by in situ hybridization and the use of microelectrodes. *Appl. Environ. Microbiol.*, **65**(7), 3182–3191.

Okabe, S., Kindaichi, T., Ito, T. and Satoh, H. (2004). Analysis of size distribution and areal cell density of ammonia-oxidizing bacterial microcolonies in relation to substrate microprofiles in biofilms. *Biotechnol. Bioeng.*, **85**(1), 86–95.

Picioreanu, C., van Loosdrecht, M.C.M. and Heijnen, J.J. (1998). Mathematical modeling of biofilm structure with a hybrid differential-discrete cellular automaton approach. *Biotechnol. Bioeng.*, **58**(1), 101–116.

Picioreanu, C., Kreft, J.U. and van Loosdrecht, M.C.M. (2004). Particle-based multidimensional multispecies biofilm model. *Appl. Environ. Microbiol.*, **70**(5), 3024–3040.

Pynaert, K., Smets, B.F., Wyffels, S., Beheydt, D., Siciliano, S.D. and Verstraete, W. (2003). Characterization of an autotrophic nitrogen-removing biofilm from a highly loaded lab-scale rotating biological contactor. *Appl. Environ. Microbiol.*, **69**(6), 3626–3635.

Schramm, A., de Beer, D., Gieseke, A. and Amann, R. (2000). Microenvironments and distribution of nitrifying bacteria in a membrane-bound biofilm. *Environ. Microbiol.*, **2**(6), 680–686.

Semmens, M.J., Dalun, K., Shanahan, J. and Christianson, A. (2003). COD and nitrogen removal by biofilms growing on gas permeable membranes. *Wat. Res.*, **37**, 4343–4350.

Terada, A., Hibiya, K., Nagai, J., Tsuneda, S. and Hirata, A. (2003). Nitrogen removal characteristics and biofilm analysis of a membrane-aerated biofilm reactor applicable to high-strength nitrogenous wastewater treatment. *J. Biosci. Bioeng.*, **95**(2), 170–178.

Wagner, M., Rath, G., Amann, R., Koops, H.P. and Schleifer, K.H. (1995). In-situ identification of ammonia-oxidizing bacteria. *Syst. Appl. Microbiol.*, **18**(2), 251–264.